ELSEVIER

Catalysis Today 67 (2001) 85–99

CATALYSIS TODAY

www.elsevier.com/locate/cattod

Effect of energy transport on a palladium-based membrane reactor for methane steam reforming process

Giuseppe Marigliano [a], Giuseppe Barbieri [a,*], Enrico Drioli [a,b]

[a] *Research Institute on Membrane and Modelling of Chemical Reactors, IRMERC-CNR, c/o University of Calabria, Via P. Bucci, 87030 Rende (CS), Italy*

[b] *Department of Chemical Engineering and Materials, University of Calabria, Via Pietro Bucci, Cubo 17/C, I-87030 Rende (CS), Italy*

Abstract

Energy transport in a Pd-based membrane reactor (MR) was analysed for an annular and a tubular configuration with a one-dimensional mathematical model. This model takes into account also the energy transfer associated to the hydrogen permeation through a Pd-based membrane. The heat required by the reaction that takes place in a tubular MR is distributed in a larger reactor length when compared to the annular MR; therefore, the heat fluxes from the oven to the reaction side is lower in a tubular MR. Outlet MR conversion is an increasing function of the temperature, sweep factor and overall heat transfer coefficient. An annular MR at 600°C reaches the maximum conversion at a reactor length lower than 1 cm. A much higher reactor length of a tubular MR is necessary to achieve the same conversion. An annular MR presents a better thermal performance and a higher conversion at a reactor length characteristic of a lab scale MR, and also its reaction path is nearer to the optimal behaviour.

Keywords: Energy transport; Equilibrium of membrane reactors; Conversion–temperature diagram; Non-isothermal model; Methane steam reforming

1. Introduction

The energy transport in any reactor has a significant effect on the temperature and as a consequence on the thermodynamics and kinetics. Energy requirement absorbed or realised during a reaction generates radial and axial temperature profiles inside the reactor. Temperature control allows carrying out the reaction in the desired conditions. The realisation of this task is not easy to realise also in a traditional reactor (TR) and its importance and complexity is higher in a membrane reactor (MR) where other profiles are present in the membrane and in the permeation stream, due to the presence of the membrane. Interaction studies among reaction enthalpy, kinetics and heat exchange with the oven and between the reaction and permeation streams are interesting.

A simple form of an MR consists of two concentric tubes, where the inner tube is the membrane and the outer one is the stainless steel shell. The catalyst can be packed in the annular space or in the core of the tube. When the catalyst is packed in the annulus the reactor will named *annular MR*; in the other case, the reactor will be indicated as *tubular MR*. The effect

Abbreviations: MR, membrane reactor; *MR*, membrane reactor path; TR, traditional reactor; *TR*, traditional reactor path; SCCM, cm^3 (TPS)/min

*Corresponding author. Tel.: +39-0984-492012; fax: +39-0984-402103.

E-mail address: g.barbieri@irmerc.cs.cnr.it (G. Barbieri).

0920-5861/01/$ – see front matter
PII: S0920-5861(01)00268-1

Nomenclature

A	membrane or heat exchange surface (cm^2)
C_p	thermal molar capacity (kJ/mol °C)
E_p	activation energy of hydrogen permeability (kJ/mol)
h	heat transfer film coefficient (W/m^2 K)
H	specific enthalpy (kJ/mol)
ΔH	heat of reaction (kJ/mol)
I	sweep factor: ratio between flow rate of sweep gas and reference component (–)
J	permeation flux (mmol/cm^2 s)
k	thermal conductivity (W/m K)
m	feed molar ratio H_2O/CH_4 (–)
N	flux (mmol/cm^2 s)
$N_{Reaction}$	number of reactions
$N_{Species}$	number of species
P	pressure (Pa)
Q	flow rate (SCCM)
Q_0	pre-exponential factor of Sivert's permeability coefficient (mmol/(cm $MPa^{0.5}$ min))
r	reaction rate (mmol/cm^3 s)
R	ideal gas constant
S	cross-section area (cm^2)
T	temperature (°C)
U	overall heat transfer coefficient between the oven and the reaction volume (W/m^2 K)
U_1	overall heat transfer coefficient between oven and annulus (W/m^2 K)
U_2	overall heat transfer coefficient between annulus and tube volume (W/m^2 K)
V	volume (cm^3)
X	conversion degree (–)

Greek letters

δ	thickness (mm)
ε	porosity (–)
$\nu_{i,j}$	stoichiometric coefficient (–)
Φ	energetic term associated to hydrogen permeation (W/cm^3)
Ψ	energy generation term by chemical reaction (W/cm^3)

Subscript

i	ith species
I	a specific value of sweep factor I
j	jth reaction

Superscript

S	support
SS	stainless steel

of the energy transport on the yields for annular and tubular MRs is very different.

A simple analysis of the behaviour of the two reactors can be performed with a relative simple one-dimensional mathematical model considering plug flow and then no radial and axial diffusion. Although this model takes into account only the axial profile, it allows to have an useful instrument to start with. This is the initial step to develop more complete models that take into account also axial and radial diffusion.

Energy transport between the energy source — the oven — and the reaction depends on the used MR configuration (annular or tubular). The heat transfer resistance for an annular MR is characteristic of the gaseous film near the stainless steel shell; the value of the overall heat transfer coefficient is of the order of 200 W/m^2 K [1]. Heat transfer resistance is located in the membrane or in its support for the tubular configuration when the catalyst is packed in the core of the tube. Thermal conductivity of the alumina and of the gases inside the porous is responsible of the global resistance for heat transfer in a Pd–Ag/Al_2O_3 supported membrane. In this case, the overall heat transfer coefficient is two order less than the previous ($\sim$2 W/m^2 K) [1].

An annular MR is characterised by a higher heat flux, which makes a reactor behaviour close to isothermal path. A higher quantity of heat can reach the reaction volume when the reaction is endothermic; on the contrary, a higher amount of heat can be removed when an exothermic reaction takes place in the MR. A tubular MR is characterised by lower heat fluxes; therefore, its behaviour tends towards to that of an adiabatic MR. Also, the control of the reaction condition is easier for an annular MR. Isothermal path is the optimal behaviour [2] for an endothermic reaction, like methane steam reforming (MSR), for example. The

optimal behaviour for an exothermic reaction is the path that follows the maximum of the reaction rate. An annular MR is the better reactor for both reaction types. In fact, in the first case a higher heat flux allows higher values of the reaction temperature, whereas in the second case there is a higher possibility to remove the generated heat. Therefore, the process can be carried out in the better conditions for both reaction types.

Annular and tubular MRs reach the same equilibrium conditions characterised also by the same conversion, if the reactor length is sufficient long; however, an annular MR reaches equilibrium conditions at much lower reactor length. In a tubular MR the lower temperature has also a significant influence on the catalytic processes; so, also the kinetics is reduced.

MSR is the considered reaction in the present work due to its significant importance for the chemical industry [3].

MSR over Ni-based catalyst [4,17] involves five species in three reversible reactions:

$$CH_4 + H_2O = CO + 3H_2, \quad \Delta H_{298} = 206\,\mathrm{kJ\,mol^{-1}} \tag{1}$$

$$CO + H_2O = CO_2 + H_2, \quad \Delta H_{298} = -41\,\mathrm{kJ\,mol^{-1}} \tag{2}$$

$$CH_4 + 2H_2O{=}CO_2 + 4H_2, \ \Delta H_{298} = 165\,\mathrm{kJ\,mol^{-1}} \tag{3}$$

High temperature and low pressure thermodynamically favour the reforming reaction (1). The second reaction does not depend on pressure and is favoured by low temperature. Heat developed by reaction (2) is not sufficient for the whole process thermal needs, as can been seen from the overall reaction (3).

This reaction is highly endothermic and characterised by fast kinetics; therefore, it required a high heat flux. The MR is more or less able to transfer the heat required by reaction depending on the configuration of the MR itself. In addition, overall heat required by a reaction in an MR is higher than that in a TR due to the conversion increase by the selective product removal.

MSR reaction is widely studied in MRs in order to demonstrate the advantages of these last where the conversion can be increased by continuous product removal, thus overcoming the limitation of thermodynamic equilibrium. Shu et al. [5] obtained, in an isothermal MR, a conversion higher than that of the equilibrium for a TR. Jorgensen et al. [6] analysed the influence of the hydrogen removal on the carbon deposition over the catalyst. Kikuchi et al. [7] studied MSR reaction in an MR using two different dense membranes obtained with electroless-plating and chemical vapour deposition techniques. An analysis of thermal effects on MSR reaction was presented by Madia et al. [1].

Several modelling works of MRs appeared recently in the literature. Itoh et al. [8,18] simulated the methylcyclohexane and 1-butene [9] dehydrogenation in a Pd MR for both parallel-flow and counter-current flow reactor configurations. Argawalla and Lund [10] performed an analysis for a consecutive reaction scheme in a concentric-tube catalytic MR. Becker et al. [11] formulated a two-dimensional mathematical model for catalytic dehydrogenation of ethylbenzene in a parallel-flow MR. Hara et al. [12] studied the effect of hydrogen removal on methanol decomposition. MSR was modelled by Oklany et al. [13,19], assuming parallel-flow in a Pd MR. A comparison [13,19] between dense and microporous MRs shows that a Pd MR gives better performance in the MSR. A computer code to simulate the isothermal behaviour of a Pd MR with retentate and permeation streams in parallel or counter-current flows was developed by Barbieri and Di Maio [14]. An analysis of MSR reaction in conversion–temperature diagram was proposed [15] in order to individuate the theoretical limits for a Pd MR.

2. System description

The MR considered was made by two concentric tubes: the outer tube was the shell, the inner one was the supported membrane. The catalyst can be packed in two different configurations (Table 1). The Pd–Ag membrane, having 7.5 μm thickness, is supported on the external surface of an Al_2O_3 porous tube (Johnson Matthey®). Inner diameter of the support is 21 mm and the outer diameter is 25 mm. Inner diameter of the shell was chosen equal to 32.6 mm in order to have the same cross section and volume for the annulus

Table 1
Membrane reactor configurations

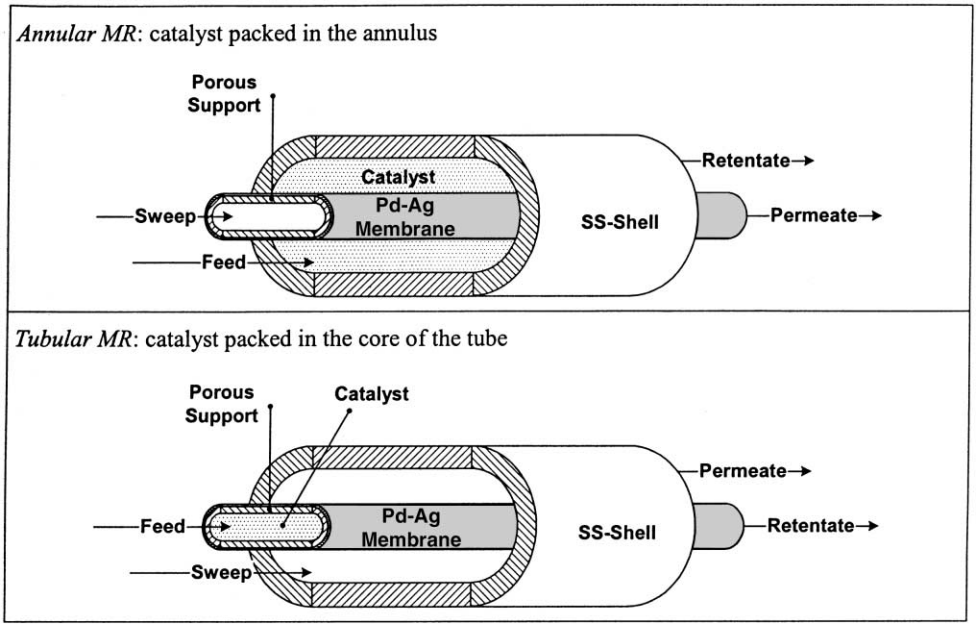

and the tube. Thus, it is possible to compare directly the results obtained for the two configurations. The amount of packed catalyst, Ni (30 wt.%) supported on alumina, is 0.5 g per 1 cm of reactor length.

The two configurations have very different behaviour, in particular for the heat exchange. The overall heat transfer coefficient U_1 between the oven and the annulus depends on the resistance in the film near the stainless steel shell. The major resistance for the heat exchange between the annulus and the tube side is the conductivity through the ceramic porous material of the tube itself. Madia et al. reported a value of 227 $W/m^2\,K$ for U_1 and of 2.4 $W/m^2\,K$, two orders lower for U_2. The heat transfer coefficient U between the oven and the reaction volume is equal to U_1 for the annular MR and is equal to $U = ((1/U_1) + (1/U_2))^{-1} \cong U_2$ for the tubular MR. Therefore, when the reaction is located in the annulus, the heat flux exchanged is high and the temperature reaction increases quickly, reaching that of the oven. On the contrary, in the tubular MR the heat transfer resistance is high and the temperature reaction remains lower than the oven temperature. As a consequence also the conversion has the same behaviour.

Table 2
Geometric parameters for the MRs and TR utilised in the simulations

	Value for the MR	Value for the TR	Unit
$A^{Membrane}$/reactor length	7.9	–	cm^2/cm
A^{Shell}/reactor length	10.2	10.2	cm^2/cm
A^{Tube}/reactor length	7.9	7.9	cm^2/cm
$S^{Annulus}$	3.45	3.45	cm^2
S^{Tube}	3.45	–	cm^2
δ^{Pd-Ag}	7.5	–	μm

Table 2 reports the geometric parameters used for the simulation of temperature and species profiles. In the simulation, the value of A^{Shell} for the TR was chosen equal to A^{Shell} for the MR in order to have the same surface for the heat transfer between oven and reaction stream.

3. Mathematical model

A mathematical model was written to describe the stationary state of a non-isothermal MR. It considers

the following hypothesis: (a) plug flow and isobaric conditions on reaction and permeation sides; (b) ideal gas behaviour; (c) ideal membrane behaviour and in particular, infinite hydrogen selectivity. Mass balance equations (Eqs. (4)–(6)) take into account the reaction and permeation through the Pd membrane:

1. Reaction side:

$$\frac{\mathrm{d}N_i}{\mathrm{d}z} = \sum_{j=1}^{N_{\mathrm{Reaction}}} \nu_{i,j} r_j - \frac{A^{\mathrm{Membrane}}}{V^{\mathrm{Reaction}}} J_i^{\mathrm{Permeate}} \tag{4}$$

2. Permeation side:

$$\frac{\mathrm{d}N_i}{\mathrm{d}z} = \frac{A^{\mathrm{Membrane}}}{V^{\mathrm{Permeation}}} J_i^{\mathrm{Permeate}} \tag{5}$$

3. Permeation flux through the Pd-based membrane:

$$J_i^{\mathrm{Permeate}} = \begin{cases} \dfrac{Q_0\, \mathrm{e}^{-E_\mathrm{p}/RT}}{\delta^{\mathrm{Pd-Ag}}} \left(\sqrt{P_{\mathrm{H_2}}^{\mathrm{Reaction}}} - \sqrt{P_{\mathrm{H_2}}^{\mathrm{Permeation}}} \right), & i = \mathrm{H_2} \\ 0, & i \neq \mathrm{H_2} \end{cases} \tag{6}$$

The value of r_j, Q_0, E_p are reported by Madia et al. [1].

The kinetics was described by assuming the Xu and Froment [4,17] equations.

Energy balance equations for both annular and tubular space are given below (Eqs. (7)–(10)):

1. Annulus side:

$$\sum_{i=1}^{N_{\mathrm{Species}}} N_i C_{p_i} \frac{\mathrm{d}T^{\mathrm{Annulus}}}{\mathrm{d}z} = \frac{U_1 A^{\mathrm{Shell}}}{V^{\mathrm{Annulus}}} (T^{\mathrm{Oven}} - T^{\mathrm{Annulus}}) - \frac{U_2 A^{\mathrm{Membrane}}}{V^{\mathrm{Annulus}}} (T^{\mathrm{Annulus}} - T^{\mathrm{Tube}}) + \Psi + \Phi \frac{A^{\mathrm{Membrane}}}{V^{\mathrm{Annulus}}} \tag{7}$$

2. Tube side:

$$\sum_{i=1}^{N_{\mathrm{Species}}} N_i C_{p_i} \frac{\mathrm{d}T^{\mathrm{Tube}}}{\mathrm{d}z} = \frac{U_2 A^{\mathrm{Membrane}}}{V^{\mathrm{Tube}}} (T^{\mathrm{Annulus}} - T^{\mathrm{Tube}}) + \Psi + \Phi \frac{A^{\mathrm{Membrane}}}{V^{\mathrm{Tube}}} \tag{8}$$

3. Heat generated by chemical reaction (Ψ):

$$\Psi = \begin{cases} \sum_{j=1}^{N_{\mathrm{Reaction}}} r_j (-\Delta H_j) & \text{on reaction side} \\ 0 & \text{on permeation side} \end{cases} \tag{9}$$

4. Enthalpy flux associated to hydrogen permeation (Φ):

$$\Phi = \begin{cases} 0 & \text{on reaction side} \\ J_{\mathrm{H_2}}^{\mathrm{Permeate}} (h_{\mathrm{H_2}}^{T^{\mathrm{Reaction}}} - h_{\mathrm{H_2}}^{T^{\mathrm{Permeation}}}) & \text{on permeation side} \end{cases} \tag{10}$$

The annulus exchanges heat with the oven and tube side, whereas the stream in the core of the tube exchanges heat only with the annular volume. The heat generated by the reaction Ψ is different from zero in Eq. (7) or (8), depending on the used configuration. The overall enthalpy of the reaction stream decreases for hydrogen permeation, whilst the enthalpy stream on the permeation side increases. These variations are taken into account, on both sides, by the changes of hydrogen flow rate. The reaction temperature does not have any variation due to hydrogen removal: hydrogen leaves the reaction stream at the reaction temperature. The system behaves as a splitting point for the reaction stream: the intensive variables cannot have any variations, while the extensive variables (like flow rate, stream enthalpy, etc.) undergo some changes.

On the contrary, extensive and intensive variables change on the permeation side. In particular, the permeation temperature undergoes a variation due to the mixing with the permeated hydrogen, which has a different temperature. The energetic term Φ associated to the hydrogen permeate is different from zero in Eq. (7) or (8), depending of the used configuration.

A scheme of the overall heat transfer coefficient is reported in Fig. 1. The enthalpy associated to the hydrogen permeation flux $J_{\mathrm{H_2}}$ is also reported in the same figure. TR simulations were performed with the same computer code setting at zero both the

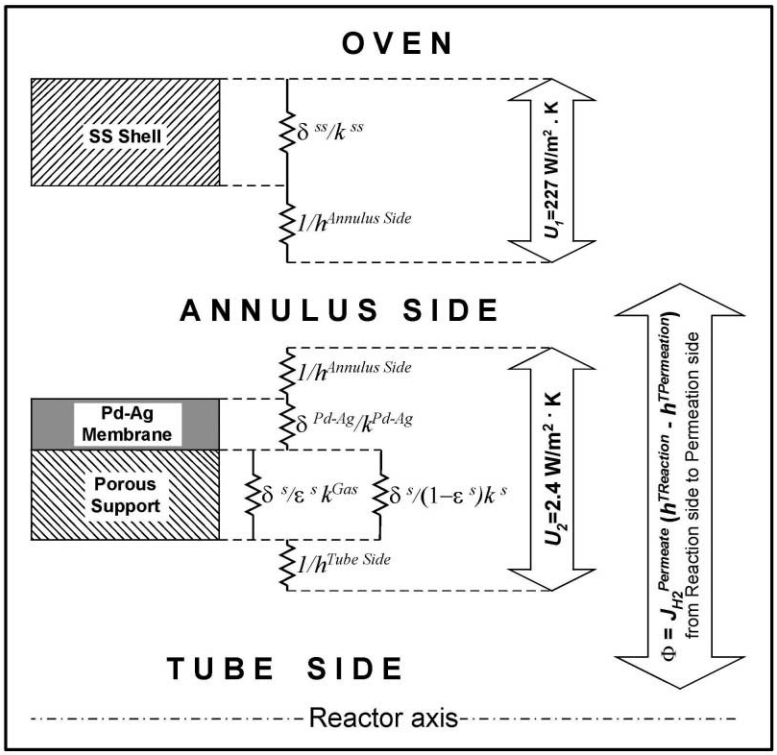

Fig. 1. Scheme of the overall heat transfer coefficients in an MR and the energy flux associated to the hydrogen permeation through Pd–Ag-based membrane.

permeating term and the overall heat transfer coefficient between the reaction and permeation side.

Thermodynamic properties used in the simulation were reported by Kee et al. [16] in the "*Chemkin thermodynamic database*".

4. Results and discussion

Equilibrium conversion of an MR [15] is an increasing function of the sweep factor I defined as the ratio between sweep gas and reference reactant flow rates. Equilibrium curve and isothermal and adiabatic reaction paths individuate a closed region, in the conversion–temperature plane: the existence region. This region includes all reaction paths starting from the same initial condition (e.g. temperature, feed molar ratio, sweep factor, etc.). Different reaction paths are followed when flow rates, membrane thickness, overall heat transfer coefficient are changed but in any case all these paths fell inside this closed region of an MR.

Therefore, the existence region defines, on one hand, the thermodynamic and, on the other side, the operative limits in which any MR operates when the initial conditions are fixed.

The MR existence region is an increasing function of the sweep factor as shown in Fig. 2, where the MR equilibrium conversion and the reactor one are reported as function of the temperature. The ratio between MR existence region for $I = 10$ ($AB_{10}C_{10}$) and the TR existence region (AB_0C_0) is about 3, and for $I = 100$ this ratio is equal to about 7.

Reaction paths for an annular and a tubular MR with $I = 10$ and 100 are also reported on the same figure. All reaction paths fall into the relative existence region; therefore, the reaction paths for an MR with a sweep factor equal to 10 fall into the existence region ($AB_{10}C_{10}$). The rate determining step between

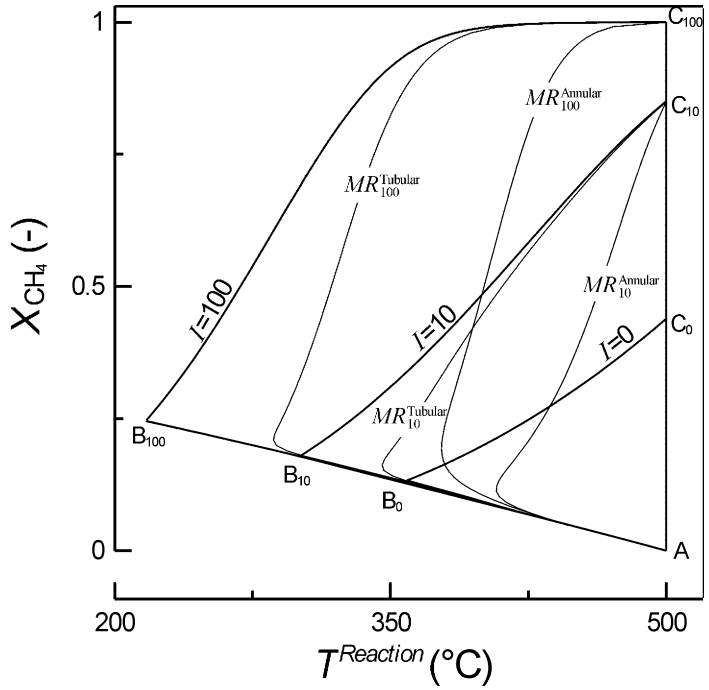

Fig. 2. Methane conversion versus temperature. Existence region of a TR (AB_0C_0) delimited by $\overline{B_0C_0}$ (equilibrium locus for $I = 0$) and $\overline{AC}_0$, $\overline{AB}_0$ (isothermal and adiabatic behaviour, respectively). Existence regions of an MR (AB_IC_I) delimited by $\overline{B_IC_I}$ (equilibrium locus for $I = 10$ and 100) and $\overline{AC}_I$, $\overline{AB}_I$ (isothermal and adiabatic reaction path, respectively). $MR_I^{Annular}$, $MR_I^{Tubular}$ reaction paths of a non-isothermal annular and tubular MR, respectively. $P^{Reaction} = P^{Permeation} = 100\,kPa$, $Q_{CH_4}^{Feed} = 200\,SCCM$, $m = 3$.

the heat transfer and the reaction plus permeation is identified following a reaction path. The temperature difference between the reaction stream and the oven can be evaluated on the horizontal line. A high value of this temperature difference is an index of a lower heat flux due to a low value of the overall heat transfer coefficient. The distance from the equilibrium line (curves $I = 0$, 10 and 100) is the driving force for the reaction and permeation. The reaction rate and the permeation driving force are higher when the distance from the equilibrium is high. In fact, when a reaction path is near to the equilibrium curve, like in the last part of the curve $MR_{100}^{Tubular}$, the reaction and permeation are very slow. Therefore, the isothermal path is the better or optimal reaction path [2] because there is no heat exchange limitation: reaction rate and permeation driving force are the highest possible at the oven temperature.

All reaction paths follow in the first part the behaviour of the adiabatic reactor and the point where they leave this path depends on the configuration and sweep factor. Thus, an annular MR leaves the adiabatic path at higher temperature with respect to a tubular MR. There is a temperature minimum, for all MRs, where the heat supplied by the oven is equal to the heat requirement of the reaction.

As can be noted, the annular MR path is closer to the optimal (isothermal) behaviour, whereas a tubular MR path is closer to the equilibrium curve confirming that the rate determining step for the last reactor is the heat transfer.

Fig. 3 [1] reports the temperature profiles for an annular and a tubular MR ($I = 10$) and a TR. The minimum temperature in the annular MR (about 405°C) is 60°C higher than the minimum temperature of the tubular MR (about 345°C). Temperature profile for a

[1] Log scale was used to expand the first part of the MR where the major changes happen. Conversion, product partial pressures and energy required by reaction are equal to zero at $z = 0$, whilst reaction and permeation temperatures are equal to oven temperature.

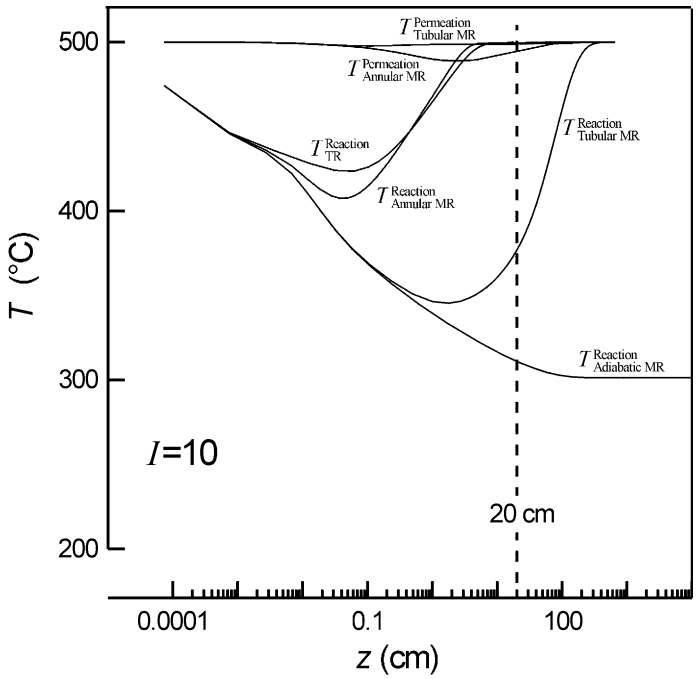

Fig. 3. Temperature profiles versus reactor length for TR and annular, tubular and adiabatic MRs. Initial conditions: $P^{\text{Reaction}} = P^{\text{Permeation}} = 100\,\text{kPa}$, $I = 10$, $m = 3$ and $Q_{CH_4}^{\text{Feed}} = 200\,\text{SCCM}$.

TR has a minimum a few degrees higher than that of an annular MR. Heat flux in the annular MR is higher due to a lower resistance and, as a consequence, the equilibrium is reached in a short reactor length. A 20 cm value for the reactor length was marked on following figures to indicate a characteristic length of a lab scale reactor. The tubular MR reaches the equilibrium at a reactor length much higher of 20 cm. In particular, the reaction temperature at 20 cm reactor length is about 375°C, much lower than the oven temperature. Therefore, higher reaction volume, amount of catalyst, etc. are necessary for a tubular MR to obtain the same performance of an annular MR.

The permeation temperature of the tubular MR has a minimum lower a few Celsius degrees than the oven temperature because the heat exchange with the oven is high. The permeation temperature of the annular MR has a minimum of about 10°C achieving the oven temperature at long reactor length. However, the reaction temperature is quite equal to the oven temperature and also the conversion has reached its maximum value, as shown in Fig. 4. An annular MR presents a much higher conversion when compared to a TR at the same reactor length. In addition, conversion level achieved by an annular MR is twice that of a TR. Conversion profile of the tubular MR follows the adiabatic conversion (that reaches the B_{10} level) and is near to this level at 20 cm of reactor length. It reaches the equilibrium conversion (level C_{10}) only at a few hundreds of centimetres of reactor length.

On the reaction side of an annular MR hydrogen partial pressure increases with the reactor length until a maximum corresponding to the maximum hydrogen permeation flux (Fig. 5). Hydrogen partial pressure decreases reaching a minimum at the same reactor length of the minimum reaction temperature; then it increases because the temperature increases achieving own equilibrium value. The permeation has a higher weight than the reaction on the hydrogen concentration also due to the reduced production rate as a consequence of the negative effect of the temperature fall on the thermodynamics and kinetics. On permeation side hydrogen partial pressure increases monotonically reaching the same value of the hydrogen partial pressure on the reaction side at a reactor length less then 20 cm. Their difference is equal to

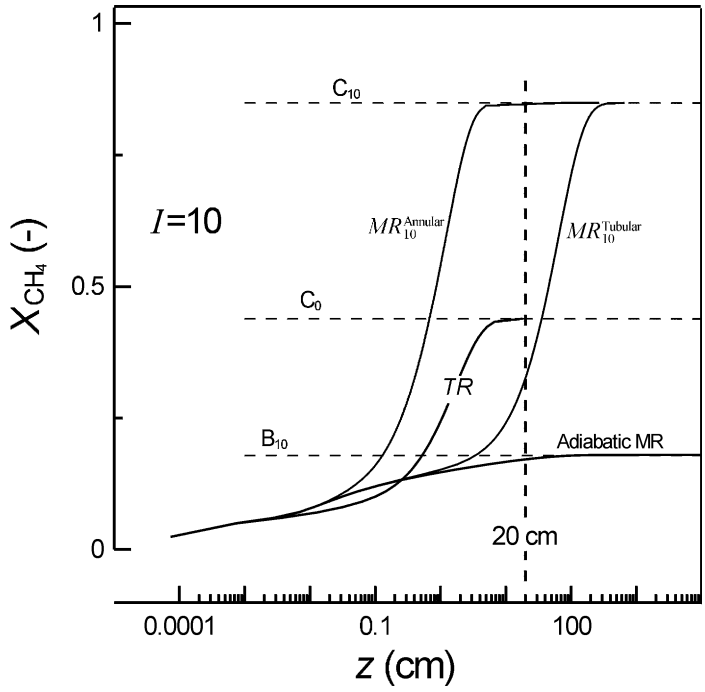

Fig. 4. Conversion degree versus reactor length for TR and annular, tubular and adiabatic MRs. Initial conditions: $P^{Reaction} = P^{Permeation} = 100\,kPa$, $I = 10$, $m = 3$ and $Q_{CH_4}^{Feed} = 200\,SCCM$.

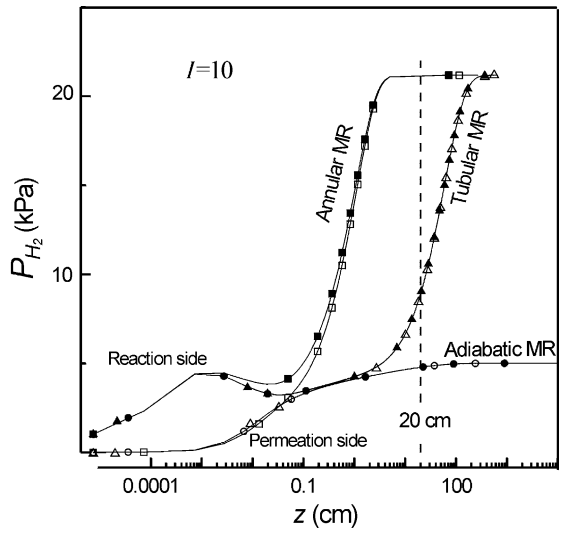

Fig. 5. Hydrogen partial pressures on reaction side for (■) annular, (▲) tubular, (●) adiabatic and on permeation side for (□) annular, (△) tubular, (○) adiabatic MRs. Operating conditions: $P^{Reaction} = P^{Permeation} = 100\,kPa$, $I = 10$, $m = 3$ and $Q_{CH_4}^{Feed} = 200\,SCCM$.

zero before the thermal equilibrium is reached as it is possible to see from Fig. 3, where the permeation temperature is not yet equal to the oven temperature. Hydrogen partial pressures of a tubular and adiabatic MRs show about the same maximum value reached by annular MR on the reaction side. Also on the permeation side they have the same behaviour until 0.5 cm of the reactor length where the difference in the partial pressures is very little. The system variation happens in conditions of permeating equilibrium: the rate determining step is the heat transfer. Hydrogen partial pressure profiles of a tubular and adiabatic MRs follow different paths in the last reactor part. Outlet hydrogen partial pressure of a tubular MR is the same of the annular MR (about 20 kPa), whereas an adiabatic MR reaches a lower value.

Temperature profiles for an MR with sweep factor of 10 and 100 have similar behaviours (Fig. 6); the energy requirements are higher for the higher conversion and then the temperature minima are lower due to a higher conversion. Reaction temperature reaches the oven temperature at lower reactor length with respect

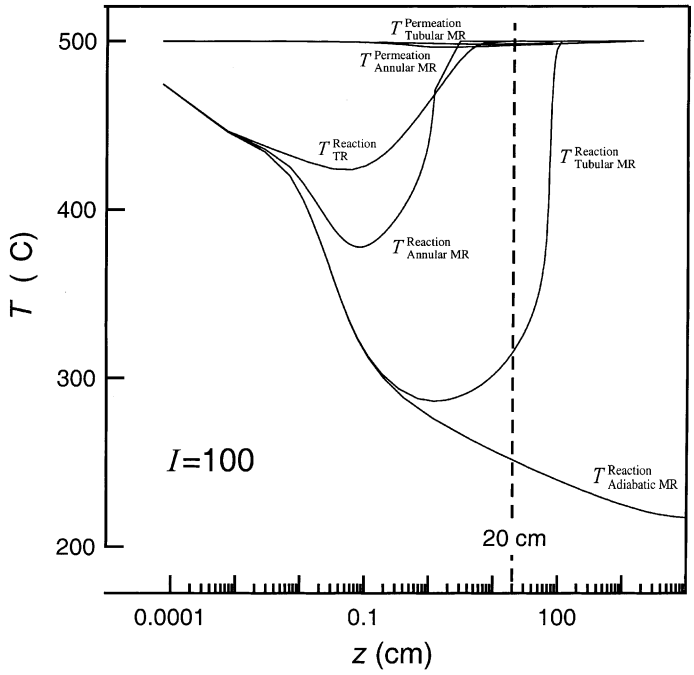

Fig. 6. Temperature profiles versus reactor length for both annular, tubular and adiabatic MRs. Initial conditions: $P^{\text{Reaction}} = P^{\text{Permeation}} = 100\,\text{kPa}$, $I = 10$, $m = 3$ and $Q_{CH_4}^{\text{Feed}} = 200\,\text{SCCM}$.

to the case $I = 10$ due to the reduced heat capacity of the reaction stream for a higher hydrogen permeation. The outlet temperature of an adiabatic MR is about 210°C; the minimum values are about 290 and 380°C for a tubular and an annular MR, respectively. Permeation temperature also for the annular MR is quite constant due to the higher heat capacity of the sweep stream of the previous case $I = 10$ about 10 times.

Equilibrium conversion for an MR is an increasing function of the sweep factor and therefore the highest level is higher than in the previous case. In particular, the maximum conversion is closed to the total conversion. Also, the adiabatic level (B_{100}) is higher when compared to the B_{10} level for $I = 10$. Conversion profiles (Fig. 7) for both annular and tubular MR, reach the maximum level (C_{100}) at lower reactor length when compared with an MR with $I = 10$: higher sweep stream removes more hydrogen produced by reaction and a lower membrane surface is necessary. Also in this case the tubular MR overcomes the characteristic reactor length of 20 cm. Conversion level reached by an MR is much higher than that of a TR (level C_0).

The slope of the conversion profiles increases with the sweep factor because residence time of the reactant stream is increased due to a higher amount of hydrogen removed from reactant stream. In fact, a TR reaches its maximum level (C_0) at 20 cm of the reactor length; at the same reactor length an MR with $I = 10$ achieves its maximum level (C_{10}), whereas when $I = 100$ the maximum level (C_{100}) is reached at 3 cm of reactor length.

Hydrogen partial pressures show (Fig. 8) the same profiles of the previous case. However, the equilibrium level (4 kPa) of hydrogen partial pressures is lower due to the higher flow rate of the sweep gas. Thus in the first reactor part, the maximum value is higher than the equilibrium value because the reaction stream has the same behaviour of the TR before that the permeation starts. These profiles were developed at lower reactor length (compared to $I = 10$) for the same reason said for the temperature and conversion profiles.

The energy required by reaction is proportional to the conversion. The overall energy required to achieve the equilibrium is higher for an MR with respect to

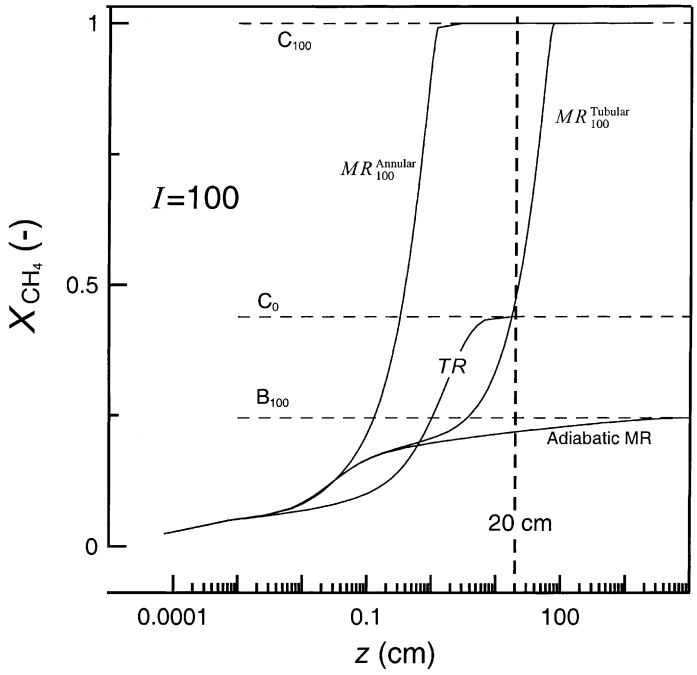

Fig. 7. Conversion degree versus reactor length for a TR and an annular, tubular and adiabatic MRs. Initial conditions: $P^{Reaction} = P^{Permeation} = 100\,kPa$, $I = 100$, $m = 3$ and $Q^{Feed}_{CH_4} = 200\,SCCM$.

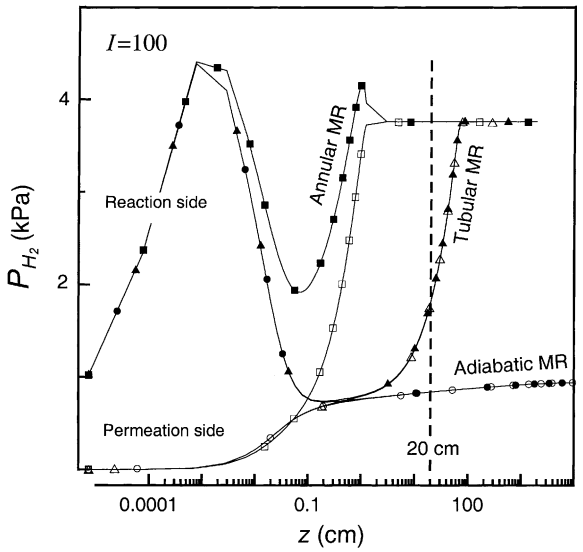

Fig. 8. Hydrogen partial pressures on reaction side for (■) annular, (▲) tubular, (●) adiabatic and on permeation side for (□) annular, (△) tubular, (○) adiabatic MRs. Operating conditions: $P^{Reaction} = P^{Permeation} = 100\,kPa$, $I = 100$, $m = 3$ and $Q^{Feed}_{CH_4} = 200\,SCCM$.

a TR due to a higher conversion; in particular, it is proportional to the C_{10} value for a non-adiabatic MR with $I = 10$, whereas for $I = 100$ it is proportional to C_{100}. Profiles of the energy required by the reaction are reported in Fig. 9. The profile of the annular MR is higher than the corresponding profile of the tubular MR in the first part and it reduces to zero at lower reactor length. Heat required by reaction is an increasing function of the sweep factor; therefore the profile for an annular MR with $I = 100$ is higher when compared to the corresponding profile for $I = 10$. However, it fell to zero at lower reactor length. The tubular MRs show same behaviour even if the heat required at a specific reactor length is lower compared to the annular MRs. However, for a tubular MR a higher reactor length is necessary to reach the equilibrium conditions.

The relative importance of the different terms, which contribute to the energy balance of the system, is reported in Figs. 10 and 11 for annular and tubular MRs. Percentages of the different terms, on the right-hand side of Eqs. (7) and (8), were calculated as ratios of the absolute value of each term by the sum of the absolute values. The energy requirement

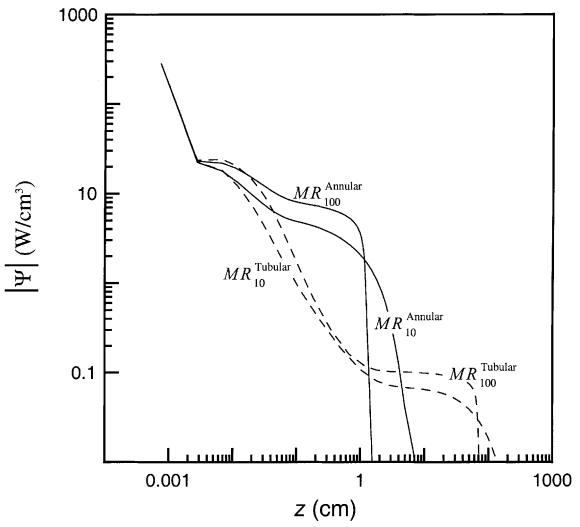

Fig. 9. Heat required by reaction (Ψ) versus reactor length for annular and tubular MR at two different sweep factor ($I = 10$ and 100). Feed conditions: $P^{\text{Reaction}} = P^{\text{Permeation}} = 100\,\text{kPa}$, $m = 3$ and $Q_{CH_4}^{\text{Feed}} = 200\,\text{SCCM}$.

by reaction Ψ is the only term different from zero at the reactor entrance; other terms are equal to zero because there is no difference in the temperatures and there is no hydrogen permeation yet. Ψ is the only important term in the first part of an annular MR. Hydrogen production increases with reaction progress therefore the relative importance of the terms related to hydrogen permeation and heat exchange increase too (Fig. 10). The Φ term assumes the maximum value in the first reactor part, where the reaction is fast, however, its importance is not relevant. This maximum is much lower than that the other terms. The heat exchange between the annulus and the oven increases and overcomes the value assumed by reaction requirements. Relative importance of the heat required by reaction decreases following the profile of the absolute value of the heat required by reaction (Fig. 10, dashed line). Simultaneously, relative importance of the heat exchanged between the annulus and permeation stream (inside the tube) $U_2(T^{\text{Reaction}} - T^{\text{Permeation}})$ increases until it assumes

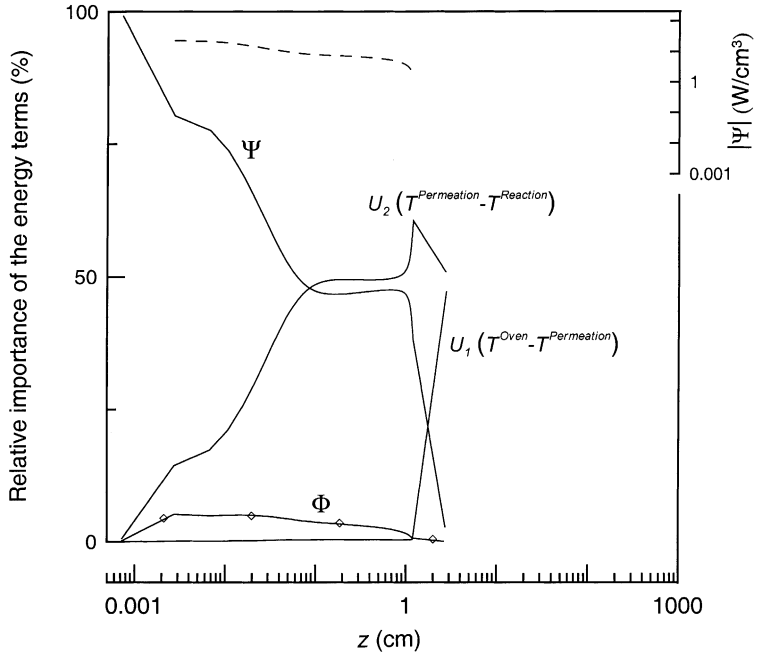

Fig. 10. Relative importance of the energy terms for an annular MR. Operating conditions: $P^{\text{Reaction}} = P^{\text{Permeation}} = 100\,\text{kPa}$, $I = 100$, $m = 3$ and $Q_{CH_4}^{\text{Feed}} = 200\,\text{SCCM}$.

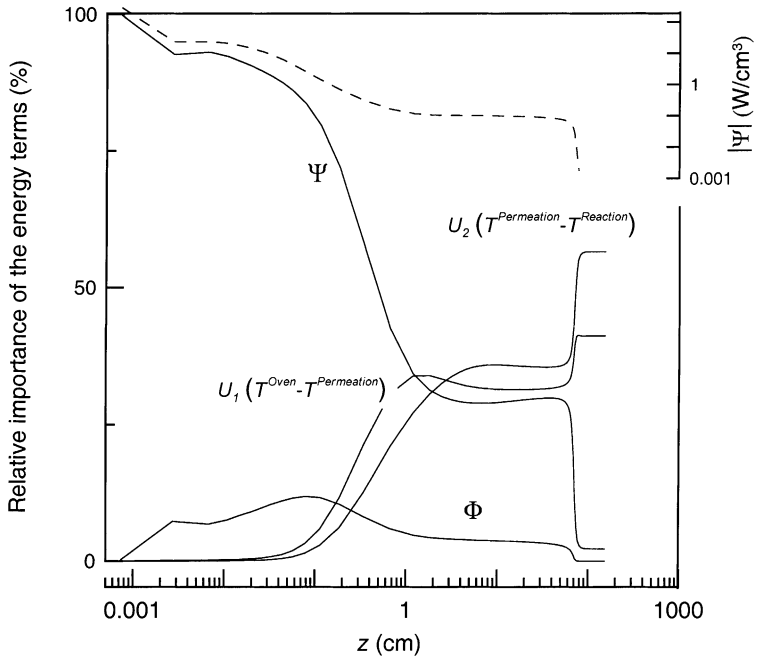

Fig. 11. Relative importance of the energy terms for tubular MR. Operating conditions: $P^{\text{Reaction}} = P^{\text{Permeation}} = 100\,\text{kPa}$, $I = 100$, $m = 3$ and $Q_{CH_4}^{\text{Feed}} = 200\,\text{SCCM}$.

a value equal to the other term of heat exchange. All terms in equilibrium condition must be equal to zero, but the numerical simulations were stopped at the achievement of these conditions $|T^{\text{Oven}} - T^{\text{Reaction}}| < 0.001$ and $|T^{\text{Oven}} - T^{\text{Permeation}}| < 0.001$. For this reason all terms are numerically different from zero at the reported reactor exit, even if their absolute values are practically reduced to zero.

The term Ψ falls down before 1 cm of the reactor length in the annular MR, whilst in the tubular MR it has a lower average (Fig. 11, dashed line) and reduces to zero at a higher reactor length. Only Ψ is important in the first part of the tubular MR (Fig. 11). The reaction temperature average is lower than the one for the annular MR due to worse heat exchange conditions. In addition, the terms of heat exchange are comparable with those relative to heat requirement by reaction. Both terms of heat exchange assume the same importance because the heat required by permeation stream is very low, thus about the total heat received (from the oven) is given to the reaction stream. The heat exchange between the annuls and the tube is higher to the energy requirement by reaction; the difference is necessary to heat the reaction stream. The energy term associated to the hydrogen permeation has a minor importance also for this configuration.

Simulations at different oven temperatures show that in all cases the annular MR has higher efficiency with respect to the tubular MR (Fig. 12). In fact, an annular MR reaches the equilibrium conversion before 20 cm of the reactor length for all oven temperatures, while the tubular MR reaches the same values at a higher reactor length.

The energy required by reaction increases with the temperature due to an increase in the equilibrium conversion. Also, the difference in the behaviour of the two proposed configurations increases with the temperature due to the difference in the overall heat transfer coefficient between the oven and reaction side. At the same reactor length, e.g. 20 cm, the difference in the conversion between the annular and tubular MRs operating at 600°C is about 0.5 much higher than the difference (0.3) of the same variable for an MR operating at 400°C.

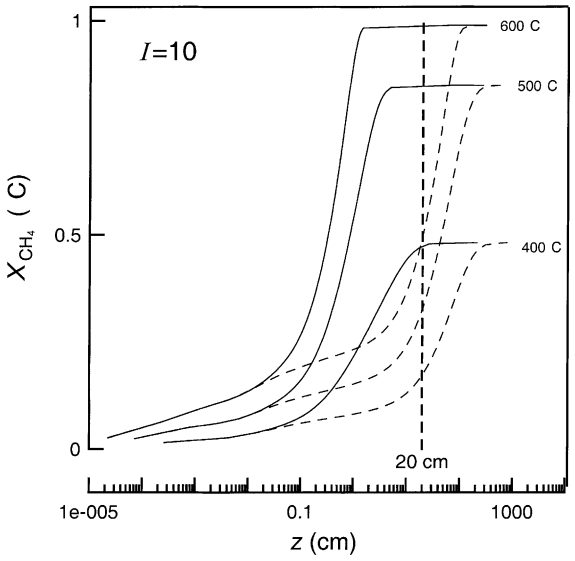

Fig. 12. Methane conversion for annular (solid lines) and tubular (dashed lines) MRs at several oven temperatures. Operating conditions: $P^{\text{Reaction}} = P^{\text{Permeation}} = 100\,\text{kPa}$, $I = 10$, $m = 3$ and $Q_{CH_4}^{\text{Feed}} = 200\,\text{SCCM}$.

5. Conclusions

Overall heat transfer coefficient U between the energy source (the oven) and the reaction volume is very different for the two proposed configurations. In particular, an annular MR has a high U value, which is two orders higher than that of a tubular MR. In the last case the major resistance is located in the porous support of the Pd membrane. Thus, the heat flux is very different between the two configurations and as a consequence the performances are also very different. The tubular MR gives the same conversion of the annular MR only at a higher reactor length, where the system equilibrium is reached. Conversion of an annular MR is much higher than conversion of a TR at any reactor length and also the maximum level is higher, more than twice for $I = 10$. Conversion of a tubular MR is lower than that of a TR and only at a higher reactor length it overcomes the equilibrium limit of the TR, achieving the same level already reached by an annular MR at lower reactor length.

Temperature profiles for both configurations decrease in the first part of reactor, reach a minimum and then increase. If the reactor length is sufficient long, the outlet temperature of a tubular MR is equal to the oven temperature. The minimum of the temperature profile is higher and it is present at lower reactor length for the annular MR due to a higher U value. A higher U value allows a higher heat flux and the heat exchange reaches and overcomes the energy required by reaction at lower reactor length, even if the heat required by reaction is higher. In an annular MR there is no rate determining step and the driving forces for heat transport and reaction plus permeation have a same order importance. Thus, heat transfer competes with reaction plus permeation until to achieve the equilibrium. Catalyst bed works better and also the membrane has a good utilisation.

Therefore, an annular MR has a better behaviour when compared to a tubular MR. In fact, it tends toward the isothermal path that is the optimal behaviour for an endothermic reaction like MSR. In addition, advantages in the use of an annular MR increases with the operating temperature.

References

[1] G.S. Madia, G. Barbieri, E. Drioli, Theoretical and experimental analysis of methane steam reforming in a membrane reactor, Can. J. Chem. Eng. 77 (1999) 698–706.
[2] O. Levenspiel, Chemical Reaction Engineering, Wiley, New York, 1972.
[3] W.H. Scholz, Process for industrial of hydrogen and associated environmental effects, Gas Sep. Purif. 7 (3) (1993) 131–139.
[4] J. Xu, G.F. Froment, Methane steam reforming methanation and water gas shift. I. Intrinsic kinetics, AIChE J. 35 (1989) 88–96.
[5] J. Shu, B.P.A. Grandjean, S. Kaliaguine, Methane steam reforming in asymmetric Pd– and Pd–Ag/porous SS membrane reactor, Appl. Catal. A 119 (1994) 305–325.
[6] S.L. Jorgensen, P.E.H. Nielsen, P. Lehrmann, Steam reforming of methane in a membrane reactor, Catal. Today 25 (1995) 303–307.
[7] E. Kikuchi, Y. Nemoto, M. Kajiwara, S. Uemiya, T. Kojima, Steam reforming of methane in membrane reactors: comparison of electroless-plating and CVD membranes and catalyst packing modes, Catal. Today 56 (2000) 75–81.
[8] N. Itoh, W.C. Xu, K. Haraya, Basic experimental study on palladium membrane reactor, J. Memb. Sci. 66 (1992) 149–155.
[9] N. Itoh, R. Govind, Combined oxidation and dehydrogenation in palladium membrane reactor, Ind. Eng. Chem. Res. 28 (1989) 1554–1557.

[10] S. Argawalla, C.R.F. Lund, Use of a membrane reactor to improve selectivity to intermediate products in consecutive catalytic reactions, J. Memb. Sci. 70 (1992) 129–141.
[11] Y.L. Becker, A.G. Dixon, W.R. Moser, Y.H. Ma, Modelling of ethylbenzene dehydrogenation in a catalytic membrane reactor, J. Memb. Sci. 77 (1993) 233–244.
[12] S. Hara, W.-C. Xu, K. Sakaki, N. Itoh, Kinetics and hydrogen removal effect for methanol decomposition, Ind. Eng. Chem. Res. 38 (1999) 488–492.
[13] J.S. Oklany, K. Hou, R. Hughes, A simulative comparison of dense microporous membrane reactors for the steam reforming of methane, Appl. Catal. A 170 (1998) 13–22.
[14] G. Barbieri, F.P. Di Maio, Simulation of the methane steam reforming process in a catalytic Pd-membrane reactor, Ind. Eng. Chem. Res. 36 (6) (1997) 2121–2127.
[15] G. Barbieri, G. Marigliano, G. Perri, E. Drioli, Conversion–temperature diagram for a palladium membrane reactor. Analysis of an endothermic reaction: methane steam reforming, Ind. Eng. Chem. Res., 2001, in press.
[16] R.J. Kee, F.M. Rupley, J.A. Miller, in: The Chemkin Thermodynamic Data Base; Sandia National Laboratories Report SAND87-8215B; Sandia National Laboratories: Albuquerque, NM, 1992.
[17] J. Xu, G.F. Froment, Methane steam reforming. II. Diffusional limitations and reactor simulation, AIChE J. 35 (1989) 97–103.
[18] N. Itoh, Development of a one-side uniform model for palladium membrane reactors, J. Chem. Eng. Jpn. 25 (3) (1992) 336–338.
[19] J.S. Oklany, E. Gobina, R. Hughes, A comparison of the performance of catalytic membrane reactors for the process of steam reforming, IChem Research Event, University of Leeds, Leeds, UK, April 1995.